Chapter 4

Renormalization group in spin glasses

The renormalization group treatment of spin glasses has long been a theoretical challenge. This chapter reviews the early standard replica symmetric description as well as the current perturbative and non-perturbative understanding of these systems.

4.1 Mean-Field and ϵ-Expansion for Spin Glasses

Tom Lubensky, Department of Physics and Astronomy, University of Pennsylvania, Philadelphia PA, USA

This section reviews my first article with Brooks Harris [1] presenting a Landau-Wilson (LW) free energy [2–6] and our follow-up work [7] about a model exhibiting transitions from the paramagnetic (P) to the ferromagnetic state (M) and from M to a spin glass (SG) in addition to a P to SG transition. This last transition was found to have an upper critical dimension, $d_c = 6$, rather than the $d_c = 4$ of familiar thermodynamic transitions. Critical exponents to first order in $\epsilon = d - d_c$ could then be obtained. The usual ϵ-expansion protocol that had been applied with great success to thermodynamic [4, 8, 9] and quantum [10, 11] phase transitions, dilute and semi-dilute polymeric solutions [12], percolation [13, 14] and branched polymers [15, 16], however, appeared not to work for SG, at least not without further tweaks. One might say that this breakdown was the *canary in a mine shaft* that provided early warning that SG models were going to require new ideas. They soon arrived in the form of replica-symmetry breaking [17] after de Almeida and Thouless demonstrated [18, 19] that the Sherrington-Kirkpatrick (SK) SG state is unstable.

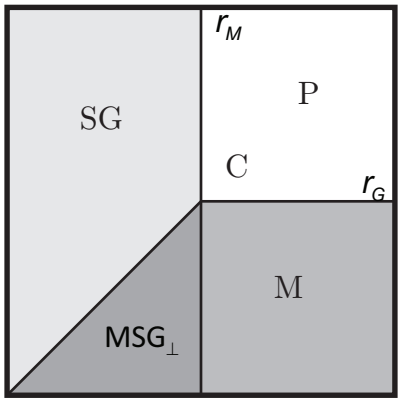

Fig. 4.1 MF phase diagram showing the P, SG, M, and $MSG_\perp$ phases and the multicritical point C. For $m = 1$, no distinct $MSG_\perp$ phase exist; it becomes part of M.

4.1.1 *Constructing a Landau-Wilson free energy*

Consider first the MF phases and phase transitions associated with the model Landau-Wilson free-energy density $\mathcal{F}$ describing a random microscopic O_m model with quenched random exchange interactions with average value, $[J]_{\rm av}$, and second cumulant $([J^2]_{\rm av} - [J]^2_{\rm av})$. $\mathcal{F}$ is a functional of the replicated [20] local magnetization $\vec{M}$ with components M_i^α and the Edwards-Anderson (EA) [20, 21] spin-glass (SG) order parameter $\overleftrightarrow{Q}$ with components $Q_{ij}^{\alpha\beta}$ with replica indices α and β running from 1 to n and O_m indices i and j running from 1 to m. The $n = 0$ procedure [22, 23] is used to produce a homogeneous energy for the random system. As usual, the diagonal elements with respect to $\alpha\beta$ of $Q_{ij}^{\alpha\beta}$ are zero, and the trace with respect to the ij indices of the off-diagonal α–β parts are equal to $[\langle\vec{S}(\mathbf{x})\rangle \cdot \langle\vec{S}(\mathbf{x})\rangle]_{\rm av}$ and are thus greater than or equal to zero. The SK model [24, 25] is a long-range version of this *local* model, which has been used, for example, in Refs. [26–28].

$\mathcal{F}$ naturally decomposes into three parts:

$$\mathcal{F} = \mathcal{F}_M + \mathcal{F}_Q + \mathcal{F}_{MQ}\,, \tag{4.1}$$

where [7]

$$\mathcal{F}_Q = \left[\frac{1}{4}r_Q \mathrm{Tr}\overleftrightarrow{Q}^2 + \frac{1}{4}\mathrm{Tr}(\nabla\overleftrightarrow{Q})^2 - w_Q \mathrm{Tr}\overleftrightarrow{Q}^3 + u_Q \mathrm{Tr}\overleftrightarrow{Q}^4 - v_Q(\mathrm{Tr}\overleftrightarrow{Q}^2)^2\right] \tag{4.2a}$$

$$\mathcal{F}_M = \left[\frac{1}{2}r_M\vec{M}\cdot\vec{M} + \frac{1}{2}\nabla_j\vec{M}\cdot\nabla_j\vec{M} + u_M\sum_\alpha M_i^\alpha M_i^\alpha M_j^\alpha M_j^\alpha - v_M(\vec{M}\cdot\vec{M})^2\right] \tag{4.2b}$$

$$\mathcal{F}_{MQ} = -w_{MQ}Q_{ij}^{\alpha\beta}M_i^\alpha M_j^\beta \tag{4.2c}$$

and where $r_Q = a_Q(T - T_Q)$ with $T_Q \sim [J^2]_{\mathrm{av}} - [J]_{\mathrm{av}}^2$ and $r_M = a_M(T - T_M)$ with $T_M \sim [J]_{\mathrm{av}}$. (The Einstein summation convention is here used.) All of the energy coefficients $w_Q, w_M, u_Q, \cdots$ except for r_Q and r_M are taken to be positive.

4.1.2 *Mean-field theory*

The MF analysis of this Landau-Wilson description captures qualitative SG features of the Edwards-Anderson (EA) [20,21] and SK [24,25] models. It produces, in particular, an essentially identical phase diagram to that of the latter.

Under the assumption that replica symmetry is not broken, both M_i^α and $Q_{ij}^{\alpha\beta}$ are independent of the indices. O_m rotational symmetry can, however, be broken leading to $\vec{M} = M\mathbf{e}$, where $\mathbf{e}$ is the m-component unit vector parallel to $\vec{M}$. The breaking of rotational symmetry by $\vec{M}$ requires the isotropy of the Edwards-Anderson SG order parameter $Q_{ij}^{\alpha\beta}$ to be broken with a component, $Q_{||}$, parallel to $\vec{M}$ and a component, $Q_\perp$, perpendicular to $\vec{M}$:

$$Q_{ij}^{\alpha\beta} = [Q_{||}e_ie_j + Q_\perp(\delta_{ij} - e_ie_j)](1 - \delta^{\alpha\beta}). \tag{4.3}$$

The $(1 - \delta^{\alpha\beta})$ factor forces all diagonal α–β components in $Q_{ij}^{\alpha\beta}$ to be zero. When M is zero, $Q_{||} = Q_\perp$ and $Q_{ij} = Q\delta_{ij}(1 - \delta^{\alpha\beta})$. The MF components of $\mathcal{F}$ are [7]

$$\mathcal{F}_M = n\left(\frac{1}{2}r_M M^2 + u_M M^4\right), \tag{4.4a}$$

$$\mathcal{F}_Q = n(n-1)\{\frac{1}{4}r_Q[(m-1)Q_\perp^2 + Q_{||}^2] - w_Q(n-2)[(m-1)Q_\perp^3 + Q_{||}^3] + \tilde{u}_Q[(m-1)Q_\perp^4 + Q_{||}^4]\}, \tag{4.4b}$$

$$\mathcal{F}_{MQ} = -n(n-1)w_{MQ}M^2Q_{||}, \tag{4.4c}$$

where $\tilde{u}_Q = (n^2 - 3n + 3)u_Q$ approaches $3u_Q$ as $n \to 0$. Note that the v_M and v_Q terms have been omitted because, being proportional to n^2, their contribution to $\mathcal{F}/n$ vanishes in the $n \to 0$ limit. The equations of state for M, $Q_{||}$, and $Q_\perp$ are

$$\frac{\partial \mathcal{F}}{n\partial M} = (r_M + 4u_M M^2 - 2(n-1)w_{MQ}Q_{||})M = 0\,, \tag{4.5a}$$

$$\frac{\partial \mathcal{F}}{n\partial Q_{||}} = (n-1)\left(\frac{1}{2}r_Q - 3(n-2)w_Q Q_{||} + 4\tilde{u}_Q Q_{||}^2\right)Q_{||} \tag{4.5b}$$

$$-(n-1)w_{MQ}M^2 = 0\,, \tag{4.5c}$$

$$\frac{\partial \mathcal{F}}{n\partial Q_\perp} = (n-1)(m-1)\left(\frac{1}{2}r_Q Q_\perp - 3(n-2)w_Q Q_\perp^2\right)Q_\perp = 0\,. \tag{4.5d}$$

Their solution determines the thermodynamic properties of M, $Q_{||}$, and $Q_\perp$ and the full phase diagram. Note that the solution to Eq. (4.5d) for $Q_\perp$ does not depend on M. An important feature of these equations is that they permit solutions with M and Q equal to zero, with $M = 0$ and $Q_{||} > 0$, and with $Q_{||}$ and M^2 greater than zero, but there is no phase with $Q_{||} = 0$ and $M \neq 0$. We will begin with a study of the SG phase in some detail and then discuss the full phase diagram.

4.1.3 *The spin-glass sector*

In the SG phase, $M = 0$, $Q_{||} = Q_\perp = Q$, and

$$Q_{ij}^{\alpha\beta} = Q\delta_{ij}(1 - \delta^{\alpha\beta}). \tag{4.6}$$

The δ_{ij} factor here implies that the pure SG state is isotropic. The LW energy for this SG state is then

$$\frac{\mathcal{F}}{mn(n-1)} = \frac{1}{4}r_Q Q^2 - w_Q(n-2)Q^3 + 4\tilde{u}_Q\, Q^4. \tag{4.7}$$

Several properties of this expression require further comment:

(1) Note the $mn(n-1)$ factor in the denominator of the right-hand side. We are interested in the limit $n \to 0$, and the normal procedure is to put the factor $(n-1)$, which is then negative, on the right side of the equation. The resulting change in the effective free-energy *equilibrium* extremum from a minimum to a maximum is unsettling. Taken at face value, the factor $n(n-1)$ is the number of degrees of freedom in the replica portion of the $\overleftrightarrow{Q}$ matrix so long as $n > 1$. An interpretation [22, 28] that avoids the extremum dilemma is to view this factor as the number

of degrees of freedom even in the analytic continuation $n \to 0$. In this interpretation, the right-hand side can be viewed as a free-energy density per degree of freedom, which has the usual property of being zero when the order parameter Q is zero and negative when r_Q becomes negative and a phase transition occurs. Unfortunately, as we shall see, the *number-of-degrees-of-freedom* interpretation presents problems when ferromagnetic as well as SG order is considered.

(2) As emphasized after Eq. (4.1), Q is constrained to be positive. The free energy in the negative half plane can therefore be ignored.

(3) There is a third-order term in Q. Normally this implies a MF first-order transition [9], in which the sign of Q in the ordered phase is opposite to that of the coefficient of Q^3 in the free-energy function. When $n > 2$, the coefficient is negative implying a first-order transition to a state of positive Q. When $n < 2$, the coefficient is positive implying a first-order transition to negative Q, which is not permitted. Rather, there is a second-order transition at $r_Q = 0$ to a state with the required positive Q. An identical behavior is noted in the treatment of percolation using the $s \to 1$ limit of the s-state Potts model [13, 14]. There, the order parameter is the (necessarily positive) probability that the diluted lattice has a connected cluster that traverses the sample in all directions. The third-order term in the Potts energy changes sign at $s = 2$, and at $s = 1$ the percolation transition is second-order with an upper critical dimension of $d_c = 6$.

Minimization of Eq. (4.7) leads to the equation of state for Q in the SG state as $r_Q \to 0$:

$$\left(\frac{1}{2}r_Q - 3(n-2)w_Q Q + 32\tilde{u}_Q Q^2\right) Q = 0\,, \tag{4.8}$$

with solution

$$\begin{aligned} Q &= \frac{1}{32\tilde{v}}\left[3(2-n)w_Q - \sqrt{[3(2-n)w_Q]^2 - 32 r_Q \tilde{u}_Q}\right] \\ &\approx \frac{r_Q}{6(2-n)w} \xrightarrow{n\to 0} -\frac{r_Q}{12 w_Q}\,, \end{aligned} \tag{4.9}$$

The contribution of the fourth-order $\tilde{u}_Q$ term to Q vanishes as $r_Q \to 0$, regardless of its sign, and near the phase transition, $Q \sim (-r_Q)^\beta$, where $\beta = 1$ rather the usual $\beta = 1/2$. The alternative solution for Q with a $+$ sign before the radical corresponds to the negative value of Q (when $n = 0$) and can be ignored. Note that the positive solution for Q emerges when $r_Q < 0$ only because the $n - 2$ term is negative when $n = 0$. If it

remained positive, a first-order rather than a second-order transition would be predicted.

4.1.4 *The full phase diagram*

The solutions to Eq. (4.5) produce the phase diagram with the P, M, SG and $\text{MSG}_\perp$ phases (Fig. 4.1). The point $\text{C} = (r_Q = 0, r_M = 0)$ is tricritical for $m = 1$ and tetracritical for $m > 1$. All of the other phase transitions are second order, so the phase boundaries are set by the vanishing of order parameters or inverse susceptibilities. The phases and their boundaries (all with $n = 0$) are then as follows.

- The paramagnetic (P) phase has the trivial solutions $M = 0$ and $Q_{||} = Q_\perp = 0$. The inverse M and SG susceptibilities are

$$\chi_M^{-1} = r_M; \qquad \chi_Q^{-1} = \chi_{Q_{||}}^{-1} = \chi_{Q_\perp}^{-1} = r_Q \,. \tag{4.10}$$

  Their zeros determine the limits of stability of the P phase and thus the PM and P-SG phases boundaries limiting P to $r_Q > 0$ and $r_M > 0$.

- The spin glass (SG) phase has $M = 0$, $r_Q < 0$, and

$$Q = Q_{||} = Q_\perp = -r_Q/12w_Q \tag{4.11}$$

  with susceptibilities

$$\chi_Q^{-1} = \chi_{Q_{||}}^{-1} = \chi_{Q_\perp}^{-1} = -\frac{1}{2} r_Q \,, \tag{4.12a}$$

$$\chi_M^{-1} = r_M - (w_{MQ}/6w_Q) r_Q \,. \tag{4.12b}$$

  These equations define the boundaries, as shown in Fig. 4.1, of the SG phase to be the P-SG boundary on the line $r_Q < 0$ for $r_M > 0$ and the M-SG boundary on the line $r_M = (w_{MQ}/6w_Q) r_Q$ for $r_M < 0$ beyond which M grows from zero. Our model does not have any $Q_\perp$-M^2 coupling, and $Q_\perp$ follows Eq. (4.11) throughout the entire region $r_Q < 0$ and is insensitive to the MSG boundary. However, there is a $Q_{||}$-M^2 coupling, and $Q_{||}$ follows Eq. (4.12a) until the M-SG boundary whereupon it changes behavior.

- The magnetic (M and $\text{MQ}_\perp$) phases both exhibit both M and $Q_{||}$ order. The $\text{MQ}_\perp$ phase additionally has $Q_\perp$. For $m = 1$, however, there is no $Q_\perp$. The M phase is then determined by the two separate equations

showing interactions between M and $Q_{||}$:

$$M^2 = (1/w_{MQ})\left(\frac{1}{2}r_Q Q_{||} + 6w_Q Q_{||}^2\right) \tag{4.13a}$$

$$Q_{||} = (w_{MQ}/24\tilde{u}w_Q)\left\{-A + [A^2 - (24\tilde{u}_M w_Q/w_{MQ})r_M]^{1/2}\right\} \tag{4.13b}$$

where $A = w_Q + (v/w_{MQ})r_Q$. Clearly, $Q_{||}$ and thus M vanish when $r_M = 0$. The P-M boundary is therefore along $r_M = 0$. When $r_M = (w_{MQ}/6w_Q)r_Q$, $\frac{1}{2}r_Q + 6w_Q Q_{||} = 0$, thus verifying that $M = 0$ on the M-SG line. Both $Q_{||}$ and M^2 must be positive in the M and MQ$_\perp$ phases. It is straightforward to see that M is nonzero for $r_M < 0$ near the boundary with the P-M phase boundary, and zero for $r_M > 0$. It is also true, albeit more complicated to show, that M^2 grows continuously from zero for displacements with positive changes, Δr_Q, to r_Q perpendicular to the M-SG boundary defined by $r_M = w_{MQ}/(6w_Q)$. For $m > 1$, $Q_\perp$ is nonzero throughout the $r_Q < 0$ subspace because there is no coupling between it and either M or $Q_{||}$.

The M and MQ$_\perp$ phases, which exhibit both $\overleftrightarrow{Q}$ and $\vec{M}$ order, present greater difficulties in interpreting the $n(n-1)$ factor that, as discussed in Sec. 4.1.3, either represents the number of degrees of freedom in $\overleftrightarrow{Q}$ or signals an energy that is maximized rather than minimized in the SG phase. In the M-SG case, the $\vec{M}$ component does not have the $n-1$ problem but the $\overleftrightarrow{Q}$ part does, making it difficult to interpret $n(n-1)$ as the number of degrees of freedom. This problem can be discerned in the expressions for fluctuation corrections to the MF response function arising from the $\mathcal{F}_{MQ}$. $\mathcal{F}_M$ contains a term $\frac{1}{2}r_M\vec{M}\cdot\vec{M}$. To one-loop order in perturbation theory, r_M experiences a correction proportional to $-(n-1)w_{MQ}^2$ at point C arising from a one-loop diagram.

4.1.5 *Critical exponents and the ϵ-expansion*

The MF order-parameter exponent β and correlation-length exponent ν determine the upper critical dimension $d = d_c$, via the relation $\beta = (1/2)(d_c - 2)\nu$. In MF, Eq. (4.9) sets $\beta = 1$, and Eq. (4.2) implies $\nu = 1/2$

Table 4.1 Exponents for the SG fixed point

Exponent	$\lambda_Q - 2$	$\nu_Q - (1/2)$	$\lambda_M - 2$	$\phi_M - 1$	η_Q	η_M	ψ_Q	ψ_M
Value	$-\frac{5m\epsilon}{3(2m-1)}$	$\frac{5\epsilon}{12(2m-1)}$	$-\frac{m\epsilon}{3(2m-1)}$	$\frac{5m\epsilon}{6(2m-1)}$	$-\frac{m\epsilon}{(2m-1)}$	0	$-\epsilon$	$\frac{7m-3}{12m-6}\epsilon$

so that $d_c = 6$. The third-order term in $\mathcal{F}$ then becomes relevant in the ϵ-expansion renormalization scheme (see Table 4.1).

The momentum-shell renormalization-group-recursion relations for an ϵ-expansion about $d = 6$ are [7]

$$\frac{dr_M}{dl} = (2-\eta_M)r_M - 4m(n-1)\frac{\tilde{w}_{MQ}^2}{(1+r_M)(1+r_Q)}\,, \tag{4.14a}$$

$$\frac{dr_Q}{dl} = (2-\eta_Q)r_Q - 36m(n-2)\frac{\tilde{w}_Q^2}{(1+r_Q)^2} - \frac{4\tilde{w}_{MQ}^2}{(1+r_M)^2} \tag{4.14b}$$

$$\frac{d\tilde{w}_Q}{dl} = \frac{1}{2}(\epsilon - 3\eta_Q)\tilde{w}_Q + 36[(n-3)m+1]\tilde{w}_Q^3 + (4/3)\tilde{w}_{MQ}^3\,, \tag{4.14c}$$

$$\frac{d\tilde{w}_{MQ}}{dl} = \frac{1}{2}(\epsilon - \eta_Q - 2\eta_M)\tilde{w}_{MQ} + 4\tilde{w}_{MQ}^3 + 12m(n-2)\tilde{w}_Q\tilde{w}_{MQ}^2\,, \tag{4.14d}$$

where $\tilde{w}_S = \sqrt{K_6}w_S$ for $S = Q, M, MQ$ ($K_d = \Omega_d/(2\pi)^d$ with Ω_d the solid angle subtended by a sphere in d dimensions).

$$\eta_Q = [12(n-2)m\tilde{w}_Q^2 + (4/3)\tilde{w}_{MQ}^2] \qquad \eta_M = (4/3)(n-1)m\tilde{w}_{MQ}^2\,. \tag{4.15}$$

The outputs of Eqs. (4.14) and (4.15) are their fixed points and the standard zoo of critical exponents. A first observation is that there are three fixed points, depicted in Fig. 4.2, in the space of $w_Q > 0$ and $w_{MQ} > 0$: the Gaussian (G) fixed point at $w_Q = w_{MQ} = 0$, the SG fixed point at $w_Q = w_Q^* > 0$, $w_{MQ} = 0$, and the M-SG-fixed point at $w_Q = w_Q^{**} > 0$, $w_{QM}^{**} > 0$. The exponents $\lambda_Q = \nu_Q^{-1}$ and $\phi_M = \phi_M\lambda_Q$, where ν_Q is the correlation length exponent for Q and ϕ_M, the crossover exponent for M, are those that govern the growth of r_Q and r_M near the P-SG transition. η_Q and η_M control the behavior of correlations of Q and M, respectively, on the P-SG transition line. Finally, ψ_Q and ψ_M are the *stability* exponents that control the behavior of w_Q and w_{MQ} near their fixed point.

Tables 4.1 and 4.2 summarize the exponents for the SG transition and the M-SG multicritical point. At the G fixed point, both $\psi_Q = \psi_M = \epsilon/2$, and $\lambda_Q = \lambda_M = 2$. The SG fixed point has $\psi_Q < 0$, and is stable with respect to changes in w_Q, indicating that it describes the transition to the

Table 4.2 Exponents for the multicritical point C

Exponent	$\lambda_+ - 2$	$\lambda_- - 2$	η_Q	η_M	ψ_Q	ψ_M
$m = 1$	$-8\epsilon/3$	$-5\epsilon/3$	$-\epsilon/3$	$-\epsilon/3$	$-\epsilon$	$-5\epsilon/3$
$m = 2$	$(-1.150 + 0.3247i)\epsilon$	$(-1.150 - 0.3247i)\epsilon$	-0.2149ϵ	-0.2451ϵ	$-\epsilon$	-1.079ϵ
$m = 3$	$-(0.9407 + 0.2539i)\epsilon$	$-(0.9407 - 0.2539i)\epsilon$	0.1960ϵ	-0.2253ϵ	$-\epsilon$	-0.8686

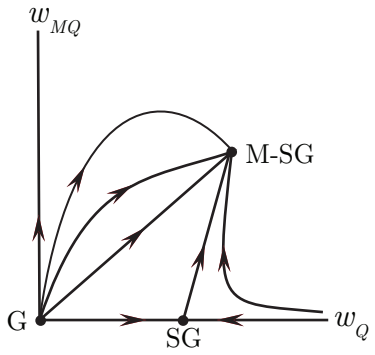

Fig. 4.2 Schematic RG flow for Eqs. (4.14) and (4.15) showing the G, SG and M-SG FP. Note that the SG FP is unstable to flow toward the M-SG one.

SG phase as long as $\vec{M}$ or w_{MQ} is zero. Because both λ_M and ψ_M are positive, both r_M and w_{QM} are relevant variables that *run away* from any initial values other than zero (see Ref. [28]). The M-SG-fixed point is the most stable one with both ψ_Q and ψ_M negative. The equations for r_Q and r_M are coupled, and, as a result, their exponents λ_+ and λ_- are associated with linear combinations of them. Curiously, λ_+ and λ_- are complex then conjugates of each other. There are other peculiarities to the RG flows even for the Ising ($m = 1$) SG case, which unlike for $m > 1$ does not have complex exponents at the M-SG fixed point.

It is therefore clear that the early and naive treatment presented in this section raises more questions than it answers. The rest of this chapter reviews the significant progress on these matters made since the 1970s.

4.2 Field theory for the Almeida-Thouless transition

Tamás Temesvári, ELTE Institute of Physics, Eötvös Loránd University, Budapest, Hungary

Imre Kondor, Complexity Science Hub, Vienna, Austria, and London Mathematical Laboratory, London, UK

MF theory is exact for the Ising spin glass on the fully connected lattice, i.e. the SK model, and its simplest solution has a transition from the paramagnet to the replica symmetric (RS) SG state in zero external field [29]. This RS phase, however, was soon proven to be unstable for zero as well as for any nonzero magnetic field whenever the temperature is low enough [30].

This instability is now understood to indicate the onset of replica symmetry breaking (RSB) in both cases. Yet the nature of the instability differs in one from the other:

- $H = 0$: The high-temperature paramagnetic phase has a unique degenerate mass m [with multiplicity $n(n-1)/2$ in the replicated theory, with n being the replica number]. The MF transition at the SG critical point $T_c^{\rm mf}$ has the character of a paramagnet to RSB SG transition, instability of the paramagnet is signaled by $m \to 0$.
- $H > 0$: The high-T phase has three different masses: replicon m_R, anomalous m_A, and longitudinal m_L. (For $n = 0$, the latter two are degenerate.) Upon lowering T, m_R vanishes at the Almeida-Thouless (AT) instability, whereas the other two modes remain noncritical. This kind of transition is now considered to be the *true* SG transition, physically resulting in the SG susceptibility to diverge, whereas the zero-field case is multicritical.

An AT transition can take place even when $H = 0$, but only for $n \gtrsim 0$ [31]. By extending the finite n calculation to $H > 0$, one can contrast the phase diagram with that for $n = 0$ (Fig. 4.3). We note the following:

(i) The finite n phase boundary has a maximum, and hence the RS phase reenters at low T.
(ii) The high-T endpoint of the finite n AT line is separated from $T_c^{\rm mf}$ by a *stable* RS SG phase.
(iii) The $T \to 0$ and $n \to 0$ limit is strongly singular: the H axis for $n = 0$ is simultaneously the innermost part of the RSB phase, and the $n \to 0$ limit of the low-T wing of the AT line.

4.2.1 *RS field theory for the AT transition*

Going beyond MF theory in d dimensions is commonly done by building an effective field theory which is suited to the calculation of perturbative corrections, and may be considered as an initial condition for iterating the renormalization group flows. For this purpose, it is usual to apply the Gaussian integral representation of the replicated and averaged partition function [32–34]:

$$\overline{Z^n} \sim \int [d\phi]\, e^{-\mathcal{L}(\phi)}\,, \qquad \mathcal{L}(\phi) = \mathcal{L}^{(G)}(\phi) + \mathcal{L}^{(I)}(\phi)$$

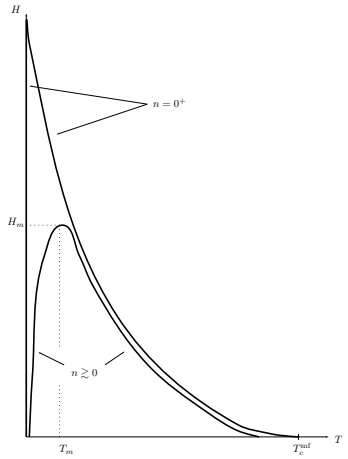

Fig. 4.3 MF phase diagram of the Ising spin glass for $n = 0^+$ and $n \gtrsim 0$. The maximum asymptotically scales as $T_m \sim n\,[\ln(n^{-2})]^{1/2}$ and $H_m \sim [\ln(n^{-2})]^{1/2}$. The low-$T$ AT line terminates at $T_{\min} \sim n\,[\ln(n^{-2})]^{-1/2}$ (not marked in the figure) for $H = 0$, signalling the RS reentrance.

with

$$\mathcal{L}^{(G)} = \frac{1}{2}\sum_{\mathbf{p}}\left[\left(\frac{1}{2}(pa\rho)^2+m_1\right)\sum_{\alpha\beta}\phi_{\mathbf{p}}^{\alpha\beta}\phi_{-\mathbf{p}}^{\alpha\beta}+m_2\sum_{\alpha\beta\gamma}\phi_{\mathbf{p}}^{\alpha\gamma}\phi_{-\mathbf{p}}^{\beta\gamma}+m_3\sum_{\alpha\beta\gamma\delta}\phi_{\mathbf{p}}^{\alpha\beta}\phi_{-\mathbf{p}}^{\gamma\delta}\right], \tag{4.16}$$

and

$$\mathcal{L}^{(I)} = -\frac{1}{3!\sqrt{N}}{\sum_{\mathbf{p_1p_2p_3}}}'\sum_{i=1}^{8} w_i\, I_i^{(3)}(\phi) - \frac{1}{4!\,N}{\sum_{\mathbf{p_1p_2p_3p_4}}}'\sum_{i=1}^{23} u_i\, I_i^{(4)}(\phi) - \ldots \tag{4.17}$$

where the fluctuating fields obey $\phi_{\mathbf{p}}^{\alpha\beta} = \phi_{\mathbf{p}}^{\beta\alpha}$ with $\phi_{\mathbf{p}}^{\alpha\alpha} = 0$, the number of the lattice sites $N \to \infty$ in the thermodynamic limit, while ρa is the interaction range. One can define the effective coordination number as $z \equiv \rho^d$. (Momentum conservation is understood in the primed sums.) The cubic and quartic RS invariants[1] in the interaction Lagrangian $\mathcal{L}^{(I)}$ have been exhibited in Refs. [34, 35], some examples are displayed below:

$$I_1^{(3)}(\phi) = \sum_{\alpha\beta\gamma}\phi_{\mathbf{p}_1}^{\alpha\beta}\phi_{\mathbf{p}_2}^{\beta\gamma}\phi_{\mathbf{p}_3}^{\gamma\alpha}\,, \quad I_2^{(3)}(\phi) = \sum_{\alpha\beta}\phi_{\mathbf{p}_1}^{\alpha\beta}\phi_{\mathbf{p}_2}^{\alpha\beta}\phi_{\mathbf{p}_3}^{\alpha\beta}\,, \quad I_3^{(3)}(\phi) = \sum_{\alpha\beta\gamma}\phi_{\mathbf{p}_1}^{\alpha\beta}\phi_{\mathbf{p}_2}^{\alpha\beta}\phi_{\mathbf{p}_3}^{\alpha\gamma}\,,$$

[1] $I_j^{(k)}$ are deemed RS invariant because they are unaffected by the global transformation $\phi'^{\alpha\beta}_{\mathbf{p}} = \phi_{\mathbf{p}}^{P_\alpha P_\beta}$, where P is any permutation of the n replicas.

and

$$I_1^{(4)} = \sum_{\alpha\beta\gamma\delta} \phi^{\alpha\beta}_{\mathbf{p}_1}\phi^{\beta\gamma}_{\mathbf{p}_2}\phi^{\gamma\delta}_{\mathbf{p}_3}\phi^{\delta\alpha}_{\mathbf{p}_4}\,, \quad I_2^{(4)} = \sum_{\alpha\beta} \phi^{\alpha\beta}_{\mathbf{p}_1}\phi^{\alpha\beta}_{\mathbf{p}_2}\phi^{\alpha\beta}_{\mathbf{p}_3}\phi^{\alpha\beta}_{\mathbf{p}_4}\,, \quad I_5^{(4)} = \sum_{\alpha\beta\gamma} \phi^{\alpha\beta}_{\mathbf{p}_1}\phi^{\alpha\beta}_{\mathbf{p}_2}\phi^{\alpha\gamma}_{\mathbf{p}_3}\phi^{\beta\gamma}_{\mathbf{p}_4}\,.$$

The stationary condition, which requires the linear term in the interaction part to vanish, gives that masses and couplings depend on temperature T, magnetic field H and replica number n, thus providing an effective field theory beyond the close vicinity of the zero-field multicritical point. One can therefore also study the $T \to 0$ regime. Exact relations further relate some couplings, the most important being $w_3 = -3w_2 = -2w_5$.

A hierarchy of the masses and couplings emerges close to $T_c^{\rm mf}$. For the paramagnet, m_1, w_1, u_1, u_2, and u_3 are the only nonzero bare parameters (up to quartic order). In the crossover region, the Lagrangian can be written as $\mathcal{L} = \mathcal{L}_{\rm para} + \delta\mathcal{L}$ with $\delta\mathcal{L}$ having additionally the parameters m_2, w_2, w_3, w_5, u_5 etc., all of which are proportional to the reduced temperature $\tau = (T_c^{\rm mf} - T)/T_c^{\rm mf}$. It is clear that the above representation of the system by the RS invariants with unrestricted replica summations and couplings belonging to them is well suited to the system close to the zero-field multicritical point where the paramagnet becomes unstable.

Close to $T = 0$, however, a new system of couplings must be chosen. We then decompose the fluctuating field as

$$\phi^{\alpha\beta}_{\mathbf{p}} = (\phi^R_{\mathbf{p}})^{\alpha\beta} + (\phi^A_{\mathbf{p}})^{\alpha\beta} + (\phi^L_{\mathbf{p}})^{\alpha\beta}$$

where

- the replicon (R) field has the property $\sum_\beta (\phi^R_{\mathbf{p}})^{\alpha\beta} = 0$ for any α, so the number of independent components is $n(n-3)/2$;
- the anomalous (A) field can be built up from $n-1$ one-replica fields $(\phi^A_{\mathbf{p}})^\alpha$ with the property $\sum_\alpha (\phi^A_{\mathbf{p}})^\alpha = 0$ as $(\phi^A_{\mathbf{p}})^{\alpha\beta} = \frac{1}{2}\big[(\phi^A_{\mathbf{p}})^\alpha + (\phi^A_{\mathbf{p}})^\beta\big]$, $\alpha \neq \beta$;
- the single component longitudinal (L) field is constant: $(\phi^L_{\mathbf{p}})^{\alpha\beta} = (\phi^L_{\mathbf{p}})$, $\alpha \neq \beta$.

$\mathcal{L}^{(G)}$ is diagonal in this new representation, whereas the cubic part of $\mathcal{L}^{(I)}$

takes the form

$$-\frac{1}{3!\sqrt{N}}\sum_{\mathbf{p_1p_2p_3}}{}' \Big\{ g_1\cdot\sum_{\alpha\beta\gamma}(\phi^R_{\mathbf{p}_1})^{\alpha\beta}(\phi^R_{\mathbf{p}_2})^{\beta\gamma}(\phi^R_{\mathbf{p}_3})^{\gamma\alpha}+\frac{1}{2}g_2\cdot\sum_{\alpha\beta}(\phi^R_{\mathbf{p}_1})^{\alpha\beta}(\phi^R_{\mathbf{p}_2})^{\alpha\beta}(\phi^R_{\mathbf{p}_3})^{\alpha\beta}$$

$$+3g_3\cdot\sum_{\alpha\beta}(\phi^R_{\mathbf{p}_1})^{\alpha\beta}(\phi^R_{\mathbf{p}_2})^{\alpha\beta}(\phi^A_{\mathbf{p}_3})^{\alpha}+3g_4\cdot\sum_{\alpha\beta}(\phi^R_{\mathbf{p}_1})^{\alpha\beta}(\phi^R_{\mathbf{p}_2})^{\alpha\beta}(\phi^L_{\mathbf{p}_3})+3g_5\cdot\sum_{\alpha\beta}(\phi^R_{\mathbf{p}_1})^{\alpha\beta}(\phi^A_{\mathbf{p}_2})^{\alpha}(\phi^A_{\mathbf{p}_3})^{\beta}$$

$$+g_6\cdot\sum_{\alpha}(\phi^A_{\mathbf{p}_1})^{\alpha}(\phi^A_{\mathbf{p}_2})^{\alpha}(\phi^A_{\mathbf{p}_3})^{\alpha}+3g_7\cdot\sum_{\alpha}(\phi^A_{\mathbf{p}_1})^{\alpha}(\phi^A_{\mathbf{p}_2})^{\alpha}(\phi^L_{\mathbf{p}_3})+g_8\cdot(\phi^L_{\mathbf{p}_1})(\phi^L_{\mathbf{p}_2})(\phi^L_{\mathbf{p}_3})\Big\}. \tag{4.18}$$

See [34] for the relation between the two sets of couplings, the g_i's and the w_i's.

To calculate corrections to MF theory near $T = 0$, we must know how the bare parameters behave in its vicinity along the MF (or tree-approximation) AT line. It is then convenient to study the $n = 0$ and $n \gtrsim 0$ cases separately (see Fig. 4.3).

- $n = 0$: The two fully-replicon cubic vertices (i.e. with all the three legs being R) diverge as

$$g_1 = g_2 \sim T^{-1}\,, \tag{4.19}$$

  whereas the others vanish like $\sim T\ln T$. Surprisingly, the longitudinal mass $m_L = m_A$ does *not* become infinitely large in this limit, instead $\lim_{T\to 0} m_L = O(1)$. Interestingly, it is not monotonic along the AT line, but has a maximum at some intermediate temperature.
- $n \gtrsim 0$: In the low temperature regime, where the $n \gtrsim 0$ line deviates from the $n = 0$ one, the two replicon vertices behave again as in Eq. (4.19). The other six vertices behave at most as $g_i \sim T^{-1}\cdot n^2$. The AT line, however, reaches the temperature axis ($H = 0$) at $T_{\min} \sim n\,[\ln(n^{-2})]^{-1/2}$, and the $n \to 0$ limit finally makes these vertices vanish.

4.2.2 *Perturbative correction to the mean field AT line*

Because perturbative considerations are somewhat modified at $d = 6$, our study in this subsection is restricted to $d > 6$.

(i) **The high-temperature endpoint of the AT line for $H = 0$:**
When both the replica number n and the magnetic field H are zero, the replicon mass is negative, $m_R = -\frac{4}{3}\,\tau^2$, thus yielding an ill-defined

replicon propagator. We must therefore resort to regularization by n or H:

- $n \gtrsim 0$ and $H = 0$. The RS phase is stable between τ_c and $\tau_{\rm AT}$, and it can also be proved that τ_c is at the same time the temperature (at one-loop level) where the paramagnet becomes unstable and the RS order parameter changes sign from negative to positive value. As for $\tau_{\rm AT}$, applying *conventional* perturbative method with $1/z \ll n \ll 0$ at one-loop order and contemplating the higher order corrections suggests the form
$$\tau_{\rm AT} = n \cdot f_1(1/nz) + n^2 \cdot f_2(1/nz) + \dots \,,$$
and by fixing z while $n \to 0$, the high-argument limit of the f functions will yield the $1/z$ expansion of $\tau_{\rm AT}(H = 0)$.
- $n = 0$ and $H^2/(kT_c^{\rm mf})^2 \gtrsim 0$. In this case, one can compute the AT temperature for a given, small magnetic field perturbatively:
$$\tau_{\rm AT} = \tau_0 + O(1/z)\,, \qquad \text{with} \qquad \tau_0 \equiv \left[\frac{3}{4}\,\frac{H^2}{(kT_c^{\rm mf})^2}\right]^{1/3} .$$
The loop expansion is generated for a given, albeit small, magnetic field with $1/z \ll \tau_0 \ll 1$. One can expect that a resummation of the whole series provides
$$\tau_{\rm AT} = \tau_0 \cdot \bar{f}(1/\tau_0 z) + \text{correction terms}\,,$$
and a nontrivial zero-field limit follows if $\lim_{u\to\infty} \bar{f}(u) \sim u$, resulting in
$$\tau_{\rm AT}(H = 0) \sim \frac{1}{z}\,,$$
in agreement with the previous regularization scheme.

(ii) **The zero-temperature limit of the AT line for $n = 0$:**
Close to $T = 0$ the loop-expansion is valid for $1/z \ll (T/T_c^{\rm mf})^2 \ll 1$, providing the result
$$\frac{H_{\rm AT}^2}{(kT_c^{\rm mf})^2} = \ln z + \ln\left(\frac{8}{9\pi}\,u\right) + O(u) \equiv \ln z + g(u) \qquad \text{with} \qquad u = \frac{1}{z}\left(\frac{T_c^{\rm mf}}{T}\right)^2 .$$
The $T = 0$ critical field is expected to be finite for a system with finite connectivity z, in contrast to the SK model. This means that $\lim_{u\to\infty} g(u)$ must be finite, providing
$$H_{\rm AT}^2(T = 0) = (kT_c^{\rm mf})^2 \cdot [\ln z + g(\infty)]\,.$$

4.2.3 *Perturbative RG for the cubic field theory*

MF theory and its perturbative corrections provide insight into the transition to the RSB phase. The renormalization group (RG) can also usually provide the correct phase diagrams and universal critical parameters for finite d, short-range systems (z finite). As discussed in Sec. 4.1, the $H = 0$ case was initially studied by Wilson's RG, which identified a stable fixed point in the first order of the ϵ-expansion, $\epsilon = 6 - d$ [36, 37]. Later works extended the calculation of the critical exponents η and ν up to third order [38]. An attempt of the RG study for the RS spin glass phase (again for $H = 0$), with the result of finding its instability, was also done in [39]. Except in this last work, a single mass m_1 and cubic coupling w_1 were considered (see Eqs. (4.16) and (4.17)), and it is the replicated paramagnet which becomes unstable on the critical surface belonging to this stable fixed point. This single critical mass is actually a direct consequence of the extra symmetry the replicated paramagnet has over the generic RS phase [35], thus resulting in the degeneracy of three different masses of the RS phase: replicon, anomalous and longitudinal [32, 39].

The *true* spin glass transition, i.e. the AT transition, has a single critical mass, namely the replicon one m_R, and only the two fully replicon cubic couplings g_1 and g_2 are different from zero (see Eq. (4.18)). The first-order RG for this three-parameter model was worked out by Bray and Roberts [33] who found no stable fixed point when $d < 6$. As for the case above $d = 6$, the stable Gaussian fixed point has, somewhat unusually, a finite basin of attraction that vanishes as $d \to 6^+$ [40]. Although not specifically examined, this finite basin of attraction may exist in any high d, and physical systems outside of it may then not be attracted by the Gaussian fixed point.

These two parts of the parameter space—the replicated paramagnet and the fully replicon subspace—are closed under the RG iteration, and are both special cases of a more general RG system with three masses and eight cubic couplings (see Eqs. (4.16), (4.17) and (4.18)). The first-order RG equations in this large parameter space were presented for generic n and for $n = 0$ in Ref. [41]. The most important conclusion from this many-parameter RG is that there is a critical AT surface in the crossover region around the zero-field fixed point over a range of dimensions $d \lesssim 6$, $d = 6$, and $d \gtrsim 6$ [42, 43]. [2] The existence of the critical AT surface around the

[2] Note that all these contributions consider a pure cubic model, which is related to but not equal with the effective field theory proposed here.

$H = 0$ fixed point does *not* contradict the lack of a stable AT-like fixed point: runaway trajectories for g_1 and g_2 are expected as the RG iterations push the system toward zero temperature.

4.2.4 *An unfinished story: transition to the RSB phase*

Stable, strong coupling fixed points Various lines of evidence support the existence of an AT-like transition in short range systems over a wide d range. Examples include the numerical work in $d = 4$ [44], Wilson's perturbative RG around the zero-field fixed point (Sec. 4.2.3), and perturbative corrections to MF theory (Sec. 4.2.2). Nevertheless, a theoretical understanding of the AT critical state is still lacking. The failure to find a stable nontrivial fixed point for $d < 6$ in the one-loop perturbative RG [33] and the runaway RG trajectories may be explained by a possible strong coupling fixed point (which is undetectable at one-loop level). Evidence for such a fixed point (stable over a range of d) has been found at two-loop level in Ref. [45], supplemented by a three-loop calculation and a resummation procedure [46], but the situation remains inconclusive (see Sec. 4.3).

Initial conditions for the RG iteration in $d > 6$ For $d > 6$ the Gaussian fixed point is stable, but its basin of attraction is finite [40]. This assessment refers to the fully replicon subspace, which is closed under the RG flow. Physical systems, however, when they are considered as initial conditions for an RG flow, usually lie outside of this subspace. It is therefore nontrivial to predict the outcome of an RG iteration. In Fig. 4.4 the AT line of the effective field theory, introduced in Sec. 4.2.1, is shown for some $d > 6$ and $1/z \ll 1$; the perturbative study in Sec. 4.2.2 is applied here. Three initial conditions on the AT line (where the exact replicon mass Γ_R is zero) are considered:

- State A: $H = 0$ endpoint of the AT line, which does not necessarily coincide with the critical point of the replicated paramagnet (see Sec. 4.2.2). This state (and those with $H \gtrsim 0$) is *far* from the fully replicon subspace, because we have (by only showing the leading terms):
$$g_1 = 1\,, \quad g_3 = -1\,, \quad g_5 = -1\,, \quad g_6 = 2\,, \quad \bar{g}_7 = -\frac{3}{2}\,, \quad \bar{g}_8 = \frac{1}{4}\,,$$
$$g_2 \sim \frac{1}{z}\,, \qquad \bar{g}_4 \sim \frac{1}{z}\,, \qquad m_R \sim -\frac{1}{z^2}\,, \qquad m_L \sim \frac{1}{z}\,;$$
see Ref. [41] for the definitions of the *bared* couplings which must be used when $n = 0$. Since $g_i/\sqrt{z} \ll 1$ for all i, this state lies inside the

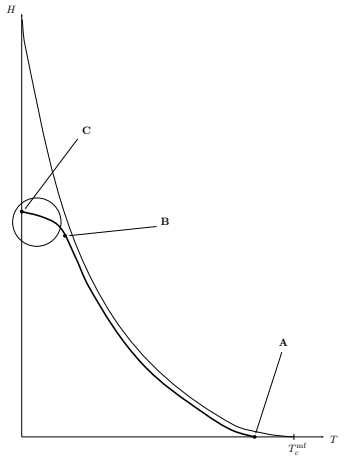

Fig. 4.4 Phase diagram of the effective field theory in the $H-T$ plane. Three states on the AT line are considered as initial conditions for the RG iteration (see text for details). The encircled region is the nonperturbative part of the RS-to-RSB transition. For comparison, the MF (tree-level) AT line is also displayed (narrow line).

perturbative region. From state A, RG iterations move the system toward the fully replicon subspace, driven by the hardening longitudinal mass ($m_L \to \infty$). Decoupling of the RG equations for g_1 and g_2 occurs when $m_L = \infty$. Although Ref. [47] supposed that the RG flow ends at the Gaussian fixed point $g_1 = g_2 = 0$ when $d \gtrsim 6$, it is difficult to see this, and a runaway flow to infinity is also conceivable.

- State B: The low-temperature end of the *perturbative* AT line where $\frac{1}{z} \ll \left(\frac{T}{T_c^{\rm mf}}\right)^2 \ll 1$. To lighten the notation, let us define $\eta \equiv \left(\frac{T}{T_c^{\rm mf}}\right)^2 \ll 1$. We have for the couplings:

$$g_1 = g_2 = \frac{4}{5}\,\eta^{-1/2} \gg 1 \qquad \text{whereas} \qquad g_3, \bar{g}_4, g_5, g_6, \bar{g}_7, \bar{g}_8 \sim \eta^{1/2} \ln \eta \ll 1.$$

  Because $g_i/\sqrt{z} \ll 1$ even for $i = 1$, 2, this initial state is still inside the perturbative regime. As for the masses, $m_L = O(1)$ and $m_R \sim -1/\eta z \ll 1$. Although this state is obviously dominated by the replicon mode, it is still somewhat outside the fully replicon subspace.
- State C: The encircled region in Fig. 4.4 shows the nonperturbative part of the AT line where $1/\eta z = O(1)$ (see Sec. 4.2.2). As for the replicon couplings, $g_1/\sqrt{z} = g_2/\sqrt{z}$ are also of order unity and we are out of the range where the perturbative RG is applicable. State C is the zero-temperature limit of the AT line where $1/\eta z \to \infty$. Considering these

infinitely large replicon couplings at $T = 0$, one can certainly conclude that, notwithstanding the correct phase diagram with the finite critical field at $T = 0$, the zero-temperature spin glass is not faithfully represented by the effective field theory put forward here. One can speculate that regularization with the replica number $n \gtrsim 0$ may remedy the problem. Alternatively, the loop expansion around the Bethe lattice (instead of the fully connected limit) at $T = 0$ may provide a solution to the problem [48].

4.3 Real-Space RG for spin glasses

Maria Chiara Angelini, Dipartimento di Fisica, Sapienza Università di Roma, Rome, Italy

As discussed in Sec. 4.2, the standard perturbative RG computation at one loop finds no suitable fixed point (FP) for $d < 6$ to describe the low-T phase [49, 50]. Although the second-order perturbative expansion finds a strong-coupling FP [46, 51], this FP is *nonperturbative*, as it cannot be reached continuously from the Gaussian one from $d_u = 6$. Given that the perturbative analysis is uncontrolled in the strong-coupling regime, the existence and relevance of this FP cannot be confirmed using the approach of Ref. [51]. Real-space RG then seem like a natural methodological choice, because the approach is non-perturbative by construction. In this section we o review the real-space RG methods that have been applied to SG, highlighting both their strengths and weaknesses.

4.3.1 *Migdal-Kadanoff RG*

Real-space RG can be viewed as a decimation procedure that reduces a larger system to a smaller one, so as to preserve–or scale appropriately–important physical observables. The partition function is then evaluated iteratively. For each iteration, a block of spins $\{\sigma\}$, described by the Hamiltonian $H(\{\sigma\})$ with couplings $\{J\}$, is replaced by an equivalent system with fewer spins $\{\sigma'\}$ and Hamiltonian $H'(\{\sigma'\})$, with renormalized couplings $\{J'\}$, such that the partition function of the original and the renormalized systems are the same. The study of the resulting transformation of the system couplings can then identify critical points and critical exponents.

While this procedure can be carried out explicitly in $d = 1$ because the Hamiltonian remains of the same form after the reduction of the degrees of freedom, for $d > 1$ new coupling terms arise between distant spins,

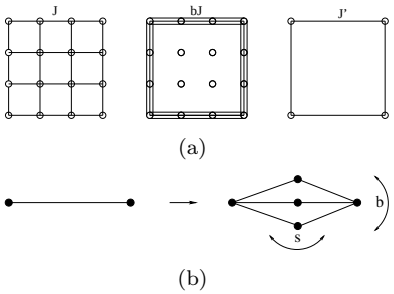

Fig. 4.5 (a) Basic step of the MK bond moving procedure to renormalize a $d = 2$ hypercubic lattice. (b) Basic step of the iterative procedure to generate a HL, for which MK RG is exact.

and the block-spin renormalization cannot be carried out exactly. The Migdal-Kadanoff (MK) approximation aims to overcome the proliferation of couplings [52,53]. Once the spins in the lattice are divided into blocks, all the couplings internal to the blocks are moved to the spins at the edges of the blocks (see Fig. 4.5(a)). An exact decimation of the spins at the edges, except those on the corners, is then performed. One can demonstrate that the free energy of the system after the bond-moving procedure is a lower bound to the free energy of the original one. The MK procedure applied to a d-dimensional hypercubic lattice consists of replacing it with a hierarchical diamond lattice (HL), for which the MK RG is exact [54]. HL are generated iteratively. The procedure starts at step $G = 0$ with two spins connected by a single link. At each step G, for each link of step $G - 1$, p parallel branches, made of s bonds in series each, are added, creating $p \cdot (s-1)$ new spins. The first step is shown in Fig. 4.5(b). The relationship between the hypercubic lattice and the associated HL is then $d = 1 + \ln(b)/\ln(s)$. The RG procedure is the exact opposite of the iterative procedure to construct the HL. For instance, in step 1, the $p \cdot (s-1)$ spins generated at the last level are integrated out, generating new effective couplings and fields between the remaining spins [3]. Particular care should be taken when fields are involved [55].

Despite its simplicity, the MK RG can capture highly nontrivial physical features. For example, it accurately describes the $T = 0$ FP of the random field Ising model [56]. However, it becomes less quantitatively accurate as d increases and sometimes even fails qualitatively [57].

[3] In the following we take $s = 2$, which is considered in all the works considered.

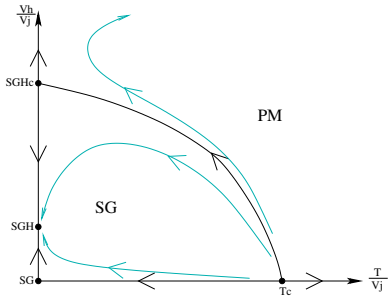

Fig. 4.6 MK RG flow in the plane $(\frac{T}{v_j} - \frac{v_h}{v_j})$ for $d > 8$. Adapted from Ref. [58].

The phase diagram for SG with $H = 0$ obtained through MK RG is depicted in Ref. [59]. The model here displays a phase transition from P to SG at $T_c(p)$. Starting at $T > T_c$, the renormalized variance of the coupling distribution v_J decreases, flowing towards the P fixed point $\frac{T}{v_j} = \infty$. Starting at $T < T_c$, the renormalized variance of the coupling distribution increases towards a $T = 0$ FP associated with the SG phase $\frac{T}{v_j} = 0$. At the SG FP, the renormalized variance of the couplings after n iterations grows as $v_J^{(n)} \propto (2^n)^\theta$. Remarkably, the dependence of θ on the effective dimension is well described by $\theta(d) = (d - 2.5)/2$, which is consistent with the lower critical dimension $d_L = 2.5$ determined numerically and theoretically [60–62].

In the SG phase, single RG trajectories are chaotic [63], and so is the renormalized couplings dependence on temperature [64]. One way out of this difficulty is to consider the contribution of random fields. Suppose that the original fields are extracted from a Gaussian distribution of zero mean and variance v_h. One can show that, for any dimension (any p), the zero temperature SG FP $\frac{T}{v_j} = 0$ becomes unstable, the external field thus corresponding to a relevant perturbation. For small enough d there is no other stable FP associated to the SG phase with field [55]. The transition seems to be destroyed by the field. However, the situation changes as d increases. The renormalization flow projected on the plane $(\frac{T}{v_j}, \frac{v_h}{v_j})$ for $d > 8$ is shown in Fig. 4.6 [58]. Even though the SG-FP is unstable also in the presence of an external field, the system then flows toward a new zero-temperature stable fixed point, SGH, which rules the behavior of the SG phase in a field. At high T and/or for strong fields the system flows to the P FP $(\frac{T}{v_j}, \frac{v_h}{v_j}) = (\infty, \infty)$. Therefore, there is necessarily an unstable

FP, SGH_c, separating the P and the SGH ones. The situation persists at $T = 0$ and governs the SG transition in a field. The fact that the critical FP point is a $T = 0$ one implies that there is a third independent critical exponent, in addition to the usual two associated with finite-T FPs. Again, one can compute the new exponent θ_c by looking at how the variance of the couplings increases at the SGH_c FP. The other consequences of a $T = 0$ FP is that, while correlation functions associated to thermal fluctuations decay as $G_{\mathrm{thermal}}(r) \propto \frac{1}{r^{d-2+\eta}}$, correlation functions associated to disordered fluctuations decay as $G_{\mathrm{disorder}}(r) \propto \frac{1}{r^{d-2+\eta-\theta_c}}$ [65]. The MK RG picture is therefore profoundly different from the standard MF description, which predicts a Gaussian FP in $d > d_u$ that is not a $T = 0$ one (see Sec. 4.1 and 4.2). For $d \to \infty$, however, the transition found through MK RG loses its $T = 0$ character because $\theta_c \to 0$. MK RG predicts a lower critical dimension $d_L = 8$, below which a stable FP cannot be found when the field is present. The same MK RG method has also been applied to models of glasses for which the microscopic degrees of freedom can take q values. Although the ensuing RG flow is similar to that in Fig. 4.6, the presence of a critical line ending on a $T = 0$ critical FP, and the low-temperature phase governed by another $T = 0$ FP, the lower critical dimension then decreases with increasing q, e.g., $d_L(q = 2) = 8$ but $d_L(q = \infty) \simeq 4$ [66, 67].

The curse of MK RG is that it assumes from the outset that the system is replica symmetric. As was shown by Gardner [68], it cannot include RSB, thus reducing the operative space to a finite, discrete space. To understand if the finite-dimensional world exhibits RSB, then RG methods are needed.

4.3.2 *Ensemble RG*

At each iteration, MK RG maps a single sample of size N to a smaller one. Given an ensemble of systems of size N, a transformation is applied to each of them to obtain an ensemble of smaller systems. However, a different approach is to establish a direct mapping between the entire probability distributions of couplings in larger and smaller systems, such that the average over such distributions of important observables remains the same. Obviously, in models for which the RG transformation is exact, the two approaches should provide the same answer, but when approximations are made, the latter could lead to better results. In particular, models with strong disorder (such as SGs), sample-to-sample fluctuations may dominate thermal ones. Following the latter approach, in Ref. [69] the Ensemble RG (ERG), was formulated.

In principle, ERG can be applied to any disordered system. However, it has so far only been applied to the hierarchical model (HM), which is a specific $d = 1$ long-range model, whose Hamiltonian for $N = 2^n$ spins can be constructed iteratively as follows:

$$H_{n+1}(s_1, ..., s_{2^{n+1}}) = H_n(s_1, ..., s_{2^n}) + H_n(s_{2^n+1}, ..., s_{2^{n+1}}) + c^{n+1} \sum_{i<j=1}^{2^{n+1}} J_{ij} s_i s_j + cost$$

In practice, H_n is the sum of interactions at n different levels. HM was introduced by Dyson in its ferromagnetic version [70,71], and its SG version was proposed in Ref. [72]. By properly tuning the factor c that controls how fast the coupling intensity decays with distance, HM can emulate a d-dimensional short-ranged (SR) model: $c \simeq 2^{-1-2/d}$ for the ferromagnetic model, $c \simeq 2^{(-1-2/d)/2}$ for the SG version (see also Ref. [73, 74]). Because decimation of HM by a standard block-spin transformation does not give rise to any multispin terms (unlike for finite-d lattices), considering pairwise interactions alone in the RG is not an approximation.

ERG assumes that couplings remain independent. They can nevertheless have a different probability distribution $P_k(J)$ at each level $k \in \{1, 2, ..., n\}$. Each coupling distribution is then parameterized by K numbers, otherwise the RG becomes untractable. For SG with a field, one can assume the distribution of couplings and fields to be two independent Gaussians, thus giving $K = 2$ parameters that are their associated variances. ERG for an ensemble of systems with n levels works as follows:

(1) Compute $(n-1)K$ observables $< O_j >$, $j \in \{K+1, ..., Kn\}$ in the larger systems extracted from the original coupling distribution.
(2) Determine the new $(n-1)K$ parameters of the P' distributions by requiring that $< O'_i >_{P'} = < O_{i+K} >_P$ for any $i \in 1, 2, ..., (n-1)K$.
(3) Build a new ensemble of systems of the original size by joining them with random couplings extracted from the original distribution $P_n(J)$ two smaller systems with couplings extracted from $P'_k(J')$, $k \in \{1, 2, ..., (n-1)\}$ found at step (2).

Primed quantities refer to the smaller systems. The first two steps are the true renormalization steps, while the last step is required to obtain a final system size that allows for iterating the method until convergence. The observables used to fix the variances in the SG ERG are normalized SG correlations at different levels. The ERG analysis of SG with $H = 0$ found a SG transition below a critical temperature for (effective) $d \simeq 3$ [69]. The method, which has been assessed by comparing with simulation results,

reproduces the proper scaling of the ν exponent, which, for long-range systems, shows a minimum at the upper critical value of c. ERG therefore correctly identifies d_u. The ERG analysis for SG in a field obtained results are in perfect agreement with what was found by MK RG [58]. The qualitative phase diagram is as in Fig. 4.6, and below $d_L \simeq 8$ ERG is unable to identify a SG phase.

4.3.3 *Strong disorder RG*

The Strong Disorder RG (SDRG) is a $T = 0$ scheme to construct an approximate SG ground state [75]. It considers the local field of each spin S_i $h_i^{loc} = \sum_j J_{ij} S_j$. Once its largest coupling (in absolute value) is computed, corresponding to some index $j_{\max}(i)$, $\max_j(|J_{ij}|) \equiv |J_{i,j_{\max}(i)}|$, one would like to identify the spins for which the local field

$$h_i^{loc} = J_{i,j_{\max}(i)} S_{j_{\max}(i)} + \sum_{j \neq j_{\max}(i)} J_{ij} S_j$$

is dominated by the first term. The second term could be approximated by a sum of random terms of absolute values J_{ij} and of random signs. It is therefore reasonable to use

$$\Omega_i \equiv |J_{i,j_{\max}(i)}| - \sqrt{\sum_{j \neq j_{\max}(i)} |J_{ij}|^2}$$

as an indicator of the relative dominance of the maximal coupling in the local field. SDRG is based on the variable Ω_i defined by the following elementary decimation scheme

(1) For each spin i, compute the associated variable Ω_i;
(2) Find the spin i_0 with the maximal Ω_i;
(3) Eliminate the spin S_{i_0}, fixing it to

$$S_{i_0} = S_{j_{\max}(i_0)} \mathrm{sgn}(J_{i_0 j_{\max}(i_0)});$$

(4) Transfer all its couplings $J_{i_0,j}$ with $j \neq j_{\max}(i_0)$ to the spin $S_{j_{\max}(i_0)}$ via the renormalization rule;

$$J^R_{j_{\max}(i_0),j} = J_{j_{\max}(i_0),j} + J_{i_0,j} \mathrm{sgn}(J_{i_0 j_{\max}(i_0)}). \tag{4.20}$$

The procedure is repeated $N - 1$ times; leaving a single spin S_{last} at the end, with $S_{last} = \pm 1$ labeling the two ground states related by a global flip of all the spins. From $S_{last} = +1$, one may reconstruct all the values of the decimated spins via the rule in Eq. (4.20), and thus approximate the energy of the ground state.

SDRG has been used to assess the validity of the Droplet Picture (DP) or Replica Symmetry Breaking (RSB) description of SG models, depending on d. In the DP, a RS low-T phase with properties determined by the excitation of droplets of fractal dimension $d_s < d$ with a free-energy cost that grows as L^θ for a length scale L. In the RSB picture, there exist system-size excitations which have a free-energy cost of O(1) and which are space-filling, i.e., have $d_s = d$. Thus, by investigating the value of d_s of interfaces in the low-T phase, it is possible to determine whether RSB or DP best describes the physics.

In SDRG, θ and d_s are obtained by considering–for each disordered sample—the two ground states associated with two different boundary conditions. Periodic (P) and Anti-Periodic (AP) conditions, in particular are obtained by flipping the sign of the bonds crossing a hyperplane of the lattice. The difference between the two ground states defines a system-size domain wall. The scaling of its energy gives θ, and the scaling of its surface gives d_s.

SDRG values for θ and d_s were first obtained for $d = 2$ and 3 [75]. While the values of d_s by SDRG are in good agreement with those obtained by numerical methods both in $d = 2$ [76] and in $d = 3$ [77], θ is not well captured, giving $\theta(d = 2) \simeq 0$. The scheme thus appears to give the opposite of MKRG, which correctly predicts θ, but misses the value of d_s which is fixed to the trivial $d_s^{MK} = d - 1$. The SDRG value of d_s up to $d = 6$, were later obtained using a greedy algorithm [78]. The two estimates appear to merge and give $d_s = d$ in $d = 6$, thus suggesting that RSB could be valid above $d = 6$, while DP could describe the model for $d < 6$.

The key problem of SDRG is that while the approach appears to be accurate for the early iterations, where there exist spins with positive (and large) Ω_i, all Ω_i eventually turn negative, a sign of a failure. As suggested by Monthus [75], it could be that the fractal dimension d_s is dominated by the early iterations, which correspond to long length scales, and for this reason, the SDGR then correctly captures its value.

4.3.4 *M-Layer expansion around the Bethe lattice solution*

We finish with a recently developed expansion around a different soluble MF model: the Bethe lattice (BL) (or, equivalently, a random regular graph of finite connectivity z). A BL model is essentially MF because of the (local) tree structure of the lattice; the contribution of finite-length loops vanishes in the thermodynamic limit. The probability distribution of a spin

is therefore independent of the probability of a nearest neighboring spin if the direct edge between them is cut. The idea of an expansion around the BL was originally introduced by Efetov [79] and revived by different authors [80, 81]. Reference [82] formalized the approach through the M-layer construction: one introduces M copies of the original finite-dimensional lattice and generates a new lattice through a local random rewiring of the links. In the $M \to \infty$ limit, the M-layer lattice is locally BL-like in that is presents a tree-like local structure without loops of finite length. (For $M = 1$, one recovers the original lattice.) Using the small parameter $1/M$, one can perform an expansion for a generic multi-point observable. The critical series is expressed as a sum of topological Feynman diagrams with the same numerical pre-factors as in field theories. The only difference is that the contribution of a given diagram must not be evaluated by associating bare propagators to its lines, as is usual; instead, one computes the observable on the corresponding topological loop diagram, thought as manually inserted in a BL. To leading order, one recovers the BL solution with no spatial loops, but upon lowering d spatial loops grow more important. They are therefore present at higher orders in the BL expansion. The perturbative nature of the BL expansion is particularly helpful in keeping computations under control. In addition, it permits following the well-threaded path of standard perturbative RG. BLRG, however, also includes non-perturbative features compared to the standard expansion. The BL solution is exact in one dimension, thus including the resummation of all the non-perturbative effects. Finite connectivity is already encoded at the 0th order of the expansion, and, consequently also accounts for important properties, such as local fluctuation of observables and heterogeneity, at variance with the expansion around the fully-connected (FC) MF solution where such effects are construed as non-perturbative effects. The M-layer expansion around BL for a SG in a field in the limit of large connectivity $z \to \infty$ (for $T > 0$) [83] recovers the standard expansion results [49, 50].

In previous sections, we have seen that non-perturbative RG schemes, such as MKRG and ERG, find a critical zero-temperature fixed point for the SG with field, for high enough d. In the FC model, the transition line in the temperature-field $(T - H)$ plane diverges at $T = 0$. There are no zero-temperature fixed points around which one could expand. By contrast, the BL presents such a transition at a finite field h_c [84], around which one can perform an expansion using the M-layer formalism. While setting the temperature straight to 0 is impossible in the Lagrangian approach of the FC expansion, $T = 0$ computations can be easily performed in the context

of the BL expansion [85]. The zero-loop two-point correlation functions and the first one-loop corrections at $T = 0$ and finite z [86] have found loop corrections not to be negligible for $d < d_u^{BL} = 8$. The upper critical dimension predicted by the BL expansion is therefore different from $d_u = 6$ predicted by standard field theory. Given that the large z results with the standard expansion finite connectivity is understood to be a crucial ingredient. In other words, the limits $z \to \infty$ and $T \to 0$ do not commute.

The natural next step is to compute three-point correlation functions associated with the cubic vertex at zero- and one-loop order for the BL expansion, to see if, by standard RG field theoretical methods, one can find a non-trivial FP of the RG equations, for $d < d_u^{BL}$. This program is currently underway.

Acknowledgments

T.L.: I am eternally grateful to have had Brooks Harris as a colleague, collaborator, and part-time mentor during the 1970s and 1980s. I am also grateful for early support from the Office of Naval Research (ONR) and for continuous support of the National Science Foundation. T.T. acknowledges financial support from the Hungarian Science Found (OTKA), No. K125171

References

[1] A. B. Harris, T. C. Lubensky and J. H. Chen, Critical properties of spin-glasses, *Physical Review Letters* **36**, pp. 415–418 (1976), doi: 10.1103/PhysRevLett.36.415.

[2] K. G. Wilson, Renormalization group and critical phenomena .1. renormalization group and kadanoff scaling picture, *Physical Review B* **4**, 9, p. 3174 (1971a), doi:10.1103/PhysRevB.4.3174.

[3] K. G. Wilson, Renormalization group and critical phenomena .2. phase-space cell analysis of critical behavior, *Physical Review B* **4**, p. 3184 (1971b), doi: I10.1103/PhysRevB.4.3184.

[4] K. G. Wilson and J. Kogut, The renormalization group and the epsilon exansion, *Physics Reports* **12C**, p. 75 (1974).

[5] A. J. Bray and M. A. Moore, Replica symmetry and massless modes in the ising spin glass, *Journal of Physics C-Solid State Physics* **12**, 1, pp. 79–104 (1979), doi:10.1088/0022-3719/12/1/020.

[6] T. Temesvari, C. De Dominicis and I. R. Pimentel, Generic replica symmetric field-theory for short range ising spin glasses, *European Physical Journal B* **25**, 3, pp. 361–372 (2002), doi:10.1140/epjb/e20020041.

[7] J. H. Chen and T. C. Lubensky, Mean field and epsilon-expansion

study of spin-glasses, *Physical Review B* **16**, pp. 2106–2114 (1977), doi: 10.1103/PhysRevB.16.2106.

[8] P. Chaikin and T. Lubensky, *Principles of Condensed Matter Physics*. Cambridge University Press (2000).

[9] N. Goldenfeld, *Lectures Phase Transitions and the Renormalization Group (Frontiers of Physics)*. Addison-Wesley (1972).

[10] J. A. Hertz, Quantum critical phenomena, *Physical Review B* **14**, pp. 1165–1184 (1976), doi:10.1103/PhysRevB.14.1165.

[11] S. Sachdev, *Quantum Phase Transitions*, 2nd edn. Cambridge University Press (2011).

[12] P. de Gennes, *Scaling concepts in Polymer Physics*. Cornell University Press (1979).

[13] P. W. Kasteleyn and F. C.M., Phase transitions in lattice systems with random local properties, *J. Phys. Soc. Jpn Suppl.* **26** (1969).

[14] A. B. Harris, T. C. Lubensky, W. K. Holcomb and C. Dasgupta, Renormalizion-group approach to percolation problems, *Physical Review Letters* **35**, 6, pp. 327–330 (1975), doi:10.1103/PhysRevLett.35.327.

[15] T. C. Lubensky and J. Isaacson, Field-theory for statistics of branched polymers, gelation, and vulcanization, *Physical Review Letters* **41**, 12, pp. 829–832 (1978), doi:10.1103/PhysRevLett.41.829.

[16] T. C. Lubensky and J. Isaacson, Statistics of lattice animals and dilute branched polymers, *Physical Review A* **20**, 5, pp. 2130–2146 (1979), doi: 10.1103/PhysRevA.20.2130.

[17] M. Mezard, G. Parisi and M. A. Virasoro, *Spin Glasses and Beyond*. World Scientific 1987 (1987).

[18] J. R. L. de Almeida and D. J. Thouless, Stability of sherrington-kirkpatrick solution of a spin glass model, *Journal of Physics a-Mathematical and General* **11**, pp. 983–990 (1978), doi:10.1088/0305-4470/11/5/028.

[19] J. R. L. de Almeida, R. C. Jones, J. M. Kosterlitz and D. J. Thouless, Infinite-ranged spin glass with m-component spins, *Journal of Physics C-Solid State Physics* **11**, pp. L871–L875 (1978), doi:10.1088/0022-3719/11/21/005.

[20] S. F. Edwards and P. W. Anderson, Theory of spin glasses, *Journal of Physics F-Metal Physics* **5**, pp. 965–974 (1975), doi:10.1088/0305-4608/5/5/017.

[21] S. F. Edwards and P. W. Anderson, Theory of spin-glasses .2, *Journal of Physics F-Metal Physics* **6**, pp. 1927–1937 (1976), doi:10.1088/0305-4608/6/10/022.

[22] V. J. Emery, Critical properties of many-component systems, *Physical Review B* **11**, pp. 239–247 (1975), doi:10.1103/PhysRevB.11.239.

[23] G. Grinstein and A. Luther, Application of renormalization group to phase-transitions in disordered systems, *Physical Review B* **13**, pp. 1329–1343 (1976), doi:10.1103/PhysRevB.13.1329.

[24] D. Sherrington and S. Kirkpatrick, Solvable model of a spin-glass, *Physical Review Letters* **35**, pp. 1792–1796 (1975), doi:10.1103/PhysRevLett.35.1792.

[25] S. Kirkpatrick and D. Sherrington, Infinite-ranged models of spin-glasses,

Physical Review B **17**, pp. 4384–4403 (1978), doi:10.1103/PhysRevB.17.4384.

[26] A. J. Bray and M. A. Moore, Replica-symmetry breaking in spin-glass theories, *Physical Review Letters* **41**, pp. 1068–1072 (1978), doi:10.1103/PhysRevLett.41.1068.

[27] A. J. Bray and M. A. Moore, Replica symmetry and massless modes in spin-glasses - 2 non-ising spins, *Journal of Physics C-Solid State Physics* **12**, pp. 1349–1361 (1979), doi:10.1088/0022-3719/12/7/023.

[28] S. Fishman and A. Aharony, Phase-diagrams and multicritical points in randomly mixed magnets .3. competing spin-glass and magnetic-ordering, *Physical Review B* **21**, pp. 280–295 (1980), doi:10.1103/PhysRevB.21.280.

[29] D. Sherrington and S. Kirkpatrick, Solvable model of a spin-glass, *Phys. Rev. Lett.* **35**, p. 1792 (1975).

[30] J. R. L. de Almeida and D. J. Thouless, Stability of the Sherrington-Kirkpatrick solution of a spin glass model, *J. Phys. A* **11**, p. 983 (1978).

[31] I. Kondor, Parisi's mean-field solution for spin glasses as an analytic continuation in the replica number, *J. Phys. A* **16**, p. L127 (1983).

[32] A. J. Bray and M. A. Moore, Replica symmetry and massless modes in the Ising spin glass, *J. Phys. C* **12**, p. 79 (1979).

[33] A. J. Bray and S. A. Roberts, Renormalisation-group approach to the spin glass transition in finite magnetic fields, *J. Phys. C* **13**, p. 5405 (1980).

[34] T. Temesvári, C. De Dominicis and I. R. Pimentel, Generic replica field-theory for short range Ising spin glasses, *Eur. Phys. J. B* **25**, p. 361 (2002).

[35] T. Temesvári, Replica symmetric spin glass field theory, *Nucl. Phys. B* **772**, 3, pp. 340–370 (2007).

[36] A. Harris, T. Lubensky and J.-H. Chen, Critical properties of spin-glasses, *Phys. Rev. Lett.* **36**, p. 415 (1976).

[37] J.-H. Chen and T. Lubensky, Mean field and ϵ-expansion study of spin glasses, *Phys. Rev. B.* **16**, p. 2106 (1977).

[38] J. E. Green, ϵ-expansion for the critical exponents of a vector spin glass, *J. Phys. A* **17**, p. L43 (1985).

[39] E. Pytte and J. Rudnick, Scaling, equation of state, and the instability of the spin-glass phase, *Phys. Rev. B.* **19**, p. 3603 (1979).

[40] M. Moore and A. Bray, Disappearance of the Almeida-Thouless line in six dimensions, *Phys. Rev. B.* **83**, p. 224408 (2011).

[41] I. R. Pimentel, T. Temesvári and C. De Dominicis, Spin-glass transition in a magnetic field: a renormalization group study, *Phys. Rev. B.* **65**, p. 224420 (2002).

[42] G. Parisi and T. Temesvári, Replica symmetry breaking in and around six dimensions, *Nucl. Phys. B* **858**, pp. 293–316 (2012).

[43] T. Temesvári, Physical observables of the ising spin glass in $6-\epsilon$ dimensions: Asymptotical behavior around the critical fixed point, *Phys. Rev. B.* **96**, p. 024411 (2017).

[44] R. A. Banos, A. Cruz, L. Fernandez, J. Gil-Narvion, A. Gordillo-Guerrero, M. Guidetti, D. Iniguez, A. Maiorano, , E. Marinari, V. Martin-Mayor, J. Monforte-Garcia, A. M. Sudupe, D. Navarro, G. Parisi, S. Perez-Gaviro,

J. Ruiz-Lorenzo, S. Schifano, B. Seoane, A. Tarancon, P. Tellez, R. Tripiccione and D. Y. J. Collaboration), Thermodynamic glass transition in a spin glass without time-reversal symmetry, *PNAS* **109**, pp. 6452–6456 (2012), (Janus Collaboration).

[45] P. Charbonneau and S. Yaida, Nontrivial critical fixed point for Replica-Symmetry-Breaking transitions, *Phys. Rev. Lett.* **118**, p. 215701 (2017).

[46] P. Charbonneau, Y. Hu, A. Raju, J. P. Sethna and S. Yaida, Morphology of renormalization-group flow for the de Almeida-Thouless-Gardner universality class, *Phys. Rev. E.* **99**, p. 022132 (2019).

[47] M. Moore and N. Read, Multicritical point on the de Almeida–Thouless line in spin glasses in $d > 6$ dimensions, *Phys. Rev. Lett.* **120**, p. 130602 (2018).

[48] M. C. Angelini, C. Lucibello, G. Parisi, G. Perrupato, F. Ricci-Tersenghi and T. Rizzo, Unexpected upper critical dimension for spin glass models in a field predicted by the loop expansion around the bethe solution at zero temperature, *Phys. Rev. Lett.* **128**, p. 075702 (2022).

[49] A. Bray and S. Roberts, Renormalisation-group approach to the spin glass transition in finite magnetic fields, *Journal of Physics C: Solid State Physics* **13**, 29, p. 5405 (1980).

[50] I. Pimentel, T. Temesvári and C. De Dominicis, Spin-glass transition in a magnetic field: A renormalization group study, *Physical Review B* **65**, 22, p. 224420 (2002).

[51] P. Charbonneau and S. Yaida, Nontrivial critical fixed point for replica-symmetry-breaking transitions, *Physical review letters* **118**, 21, p. 215701 (2017).

[52] L. P. Kadanoff, Variational principles and approximate renormalization group calculations, *Physical Review Letters* **34**, 16, p. 1005 (1975).

[53] A. A. Migdal, Phase transitions in gauge and spin-lattice systems, *Soviet Journal of Experimental and Theoretical Physics* **42**, p. 743 (1976).

[54] A. N. Berker and S. Ostlund, Renormalisation-group calculations of finite systems: order parameter and specific heat for epitaxial ordering, *Journal of Physics C: Solid State Physics* **12**, 22, p. 4961 (1979).

[55] B. Drossel, H. Bokil and M. Moore, Spin glasses without time-reversal symmetry and the absence of a genuine structural glass transition, *Physical Review E* **62**, 6, p. 7690 (2000).

[56] M. Cao and J. Machta, Migdal-kadanoff study of the random-field ising model, *Physical Review B* **48**, 5, p. 3177 (1993).

[57] F. Antenucci, A. Crisanti and L. Leuzzi, Critical study of hierarchical lattice renormalization group in magnetic ordered and quenched disordered systems: Ising and blume–emery–griffiths models, *Journal of Statistical Physics* **155**, 5, pp. 909–931 (2014).

[58] M. C. Angelini and G. Biroli, Spin glass in a field: A new zero-temperature fixed point in finite dimensions, *Phys. Rev. Lett.* **114**, 9, p. 095701 (2015).

[59] B. Southern and A. Young, Real space rescaling study of spin glass behaviour in three dimensions, *Journal of Physics C: Solid State Physics* **10**, 12, p. 2179 (1977).

[60] S. Franz, G. Parisi and M.A. Virasoro, Interfaces and louver critical dimen-

sion in a spin glass model, *J. Phys. I France* **4**, 11, pp. 1657–1667 (1994), doi:10.1051/jp1:1994213, https://doi.org/10.1051/jp1:1994213.

[61] S. Boettcher, Stiffness of the edwards-anderson model in all dimensions, *Phys. Rev. Lett.* **95**, p. 197205 (2005), doi:10.1103/PhysRevLett.95.197205, https://link.aps.org/doi/10.1103/PhysRevLett.95.197205.

[62] A. Maiorano and G. Parisi, Support for the value 5/2 for the spin glass lower critical dimension at zero magnetic field, *Proceedings of the National Academy of Sciences* **115**, 20, pp. 5129–5134 (2018).

[63] S. R. McKay, A. N. Berker and S. Kirkpatrick, Spin-glass behavior in frustrated ising models with chaotic renormalization-group trajectories, *Physical Review Letters* **48**, 11, p. 767 (1982).

[64] M. Nifle and H. Hilhorst, New critical-point exponent and new scaling laws for short-range ising spin glasses, *Physical review letters* **68**, 20, p. 2992 (1992).

[65] A. Bray and M. Moore, Scaling theory of the random-field ising model, *Journal of Physics C: Solid State Physics* **18**, 28, p. L927 (1985).

[66] M. C. Angelini and G. Biroli, Real space renormalization group theory of disordered models of glasses, *Proceedings of the National Academy of Sciences* **114**, 13, pp. 3328–3333 (2017a).

[67] M. C. Angelini and G. Biroli, Real space migdal–kadanoff renormalisation of glassy systems: recent results and a critical assessment, *Journal of Statistical Physics* **167**, 3, pp. 476–498 (2017b).

[68] Gardner, E., A spin glass model on a hierarchical lattice, *J. Phys. France* **45**, 11, pp. 1755–1763 (1984), doi:10.1051/jphys:0198400450110175500, https://doi.org/10.1051/jphys:0198400450110175500.

[69] M. C. Angelini, G. Parisi and F. Ricci-Tersenghi, Ensemble renormalization group for disordered systems, *Phys. Rev. B* **87**, 13, p. 134201 (2013).

[70] F. J. Dyson, Existence of a phase-transition in a one-dimensional ising ferromagnet, *Communications in Mathematical Physics* **12**, 2, pp. 91–107 (1969).

[71] Y. Meurice, Nonlinear aspects of the renormalization group flows of dyson's hierarchical model, *Journal of Physics A: Mathematical and Theoretical* **40**, 23, p. R39 (2007).

[72] S. Franz, T. Jörg and G. Parisi, Overlap interfaces in hierarchical spin-glass models, *Journal of Statistical Mechanics: Theory and Experiment* **2009**, 02, p. P02002 (2009).

[73] M. C. Angelini, G. Parisi and F. Ricci-Tersenghi, Relations between short-range and long-range ising models, *Physical Review E* **89**, 6, p. 062120 (2014).

[74] R. Banos, L. Fernandez, V. Martin-Mayor and A. Young, Correspondence between long-range and short-range spin glasses, *Physical Review B* **86**, 13, p. 134416 (2012).

[75] C. Monthus, Fractal dimension of spin-glasses interfaces in dimension d= 2 and d= 3 via strong disorder renormalization at zero temperature, *Fractals* **23**, 04, p. 1550042 (2015).

[76] H. Khoshbakht and M. Weigel, Domain-wall excitations in the two-dimensional ising spin glass, *Physical Review B* **97**, 6, p. 064410 (2018).

[77] W. Wang, J. Machta, H. Munoz-Bauza and H. G. Katzgraber, Number of thermodynamic states in the three-dimensional edwards-anderson spin glass, *Physical Review B* **96**, 18, p. 184417 (2017).

[78] W. Wang, M. Moore and H. G. Katzgraber, Fractal dimension of interfaces in edwards-anderson spin glasses for up to six space dimensions, *Physical Review E* **97**, 3, p. 032104 (2018).

[79] K. Efetov, Effective medium approximation in the localization theory: Saddle point in a lagrangian formulation, *Physica A: Statistical Mechanics and its Applications* **167**, 1, pp. 119–131 (1990), doi:https://doi.org/10.1016/0378-4371(90)90046-U, https://www.sciencedirect.com/science/article/pii/037843719090046U.

[80] G. Parisi and F. Slanina, Loop expansion around the bethe–peierls approximation for lattice models, *Journal of Statistical Mechanics: Theory and Experiment* **2006**, 02, pp. L02003–L02003 (2006), doi:10.1088/1742-5468/2006/02/l02003, https://doi.org/10.1088/1742-5468/2006/02/l02003.

[81] V. E. Sacksteder, Sums over geometries and improvements on the mean field approximation, *Phys. Rev. D* **76**, p. 105032 (2007), doi:10.1103/PhysRevD.76.105032, https://link.aps.org/doi/10.1103/PhysRevD.76.105032.

[82] A. Altieri, M. C. Angelini, C. Lucibello, G. Parisi, F. Ricci-Tersenghi and T. Rizzo, Loop expansion around the bethe approximation through the m-layer construction, *Journal of Statistical Mechanics: Theory and Experiment* **2017**, 11, p. 113303 (2017).

[83] M. C. Angelini, G. Parisi and F. Ricci-Tersenghi, One-loop topological expansion for spin glasses in the large connectivity limit, *EPL (Europhysics Letters)* **121**, 2, p. 27001 (2018).

[84] G. Parisi, F. Ricci-Tersenghi and T. Rizzo, Diluted mean-field spin-glass models at criticality, *Journal of Statistical Mechanics: Theory and Experiment* **2014**, 4, p. P04013 (2014).

[85] M. C. Angelini, C. Lucibello, G. Parisi, F. Ricci-Tersenghi and T. Rizzo, Loop expansion around the bethe solution for the random magnetic field ising ferromagnets at zero temperature, *Proceedings of the National Academy of Sciences* **117**, 5, pp. 2268–2274 (2020).

[86] M. C. Angelini, C. Lucibello, G. Parisi, G. Perrupato, F. Ricci-Tersenghi and T. Rizzo, Unexpected upper critical dimension for spin glass models in a field predicted by the loop expansion around the bethe solution at zero temperature, *Physical Review Letters* **128**, 7, p. 075702 (2022).